

Alma Mater Studiorum Università di Bologna
Archivio istituzionale della ricerca

Photophysical and Electrochemiluminescence of Coumarin-Based Oxazaborines

This is the final peer-reviewed author's accepted manuscript (postprint) of the following publication:

Published Version:

Mikysek T., Nikolaou P., Kafexholli M., Simunek P., Vana J., Markova A., et al. (2020). Photophysical and Electrochemiluminescence of Coumarin-Based Oxazaborines. CHEMELECTROCHEM, 7(7), 1550-1557 [10.1002/celc.201902102].

Availability:

This version is available at: <https://hdl.handle.net/11585/764745> since: 2021-03-01

Published:

DOI: <http://doi.org/10.1002/celc.201902102>

Terms of use:

Some rights reserved. The terms and conditions for the reuse of this version of the manuscript are specified in the publishing policy. For all terms of use and more information see the publisher's website.

This item was downloaded from IRIS Università di Bologna (<https://cris.unibo.it/>).
When citing, please refer to the published version.

(Article begins on next page)

This is the final peer-reviewed accepted manuscript of:

T. Mikysek, P. Nikolaou, M. Kafexholli, P. Šimůnek, J. Váňa, A. Marková, M. Vala, G. Valenti, Photophysical and Electrochemiluminescence of Coumarin-Based Oxazaborines, ChemElectroChem, 2020, 7(7), 1550-1557 The final published version is available online at: <http://dx.doi.org/10.1002/celc.201902102>

Rights / License:

The terms and conditions for the reuse of this version of the manuscript are specified in the publishing policy. For all terms of use and more information see the publisher's website.

This item was downloaded from IRIS Università di Bologna (<https://cris.unibo.it/>)

When citing, please refer to the published version.

Photophysical and Electrochemiluminescence of novel coumarin-based oxazaborines

Tomáš Mikysek,^[b] Pavlos Nikolaou,^[a] Mirjeta Kafexholli,^[c] Petr Šimůnek,^[c] Jiří Váňa,^[c] Aneta Marková,^[d] Martin Vala,^[d] and Giovanni Valenti,^{*[a]}

[a] Mr. Pavlos Nikolaou, Dr. Giovanni Valenti.
Department of Chemistry "G. Ciamician"
University of Bologna, Via Selmi 2, 40126, Bologna (Italy)
E-mail: g.valenti@unibo.it

[b] Dr. Tomáš Mikysek
Department of Analytical Chemistry
Faculty of Chemical Technology, University of Pardubice
Studentská 573, CZ-53210 Pardubice, Czech Republic

[c] Ms. Mirjeta Kafexholli, Dr. Petr Šimůnek, Dr. Jiří Váňa
Institute of Organic Chemistry and Technology, Faculty of Chemical Technology, University of Pardubice, Pardubice, Studentská 573, CZ-53210, Czech Republic

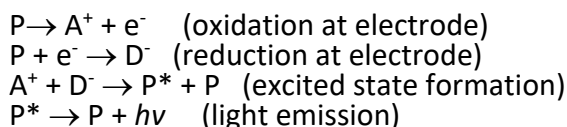
[d] Assoc. prof. Martin Vala, Ms. Aneta Marková
Brno University of Technology, Faculty of Chemistry, Materials Research Centre, Purkyňova 118, 612 00 Brno, Czech Republic

Abstract: We describe the synthesis, electrochemistry, photophysics, computational analysis and electrochemiluminescence (ECL) of a new series of oxazaborine molecules. Our strategy is based on the modification of coumarin-oxazaborine moiety to be directly joined, through carbon-carbon bond, and form donor–acceptor (D-A) chromophores. These new structures substantially change the electron distribution as well as photophysical and electrochemical behavior with a strong effect on the final quantum yield. For all compounds, we observed a very high PL quantum yield (70–75%) and relatively accessible first oxidation and first reduction. All these characteristics allows us to study the ECL of these molecules obtaining very high ECL efficiency, four times higher than the standard dyes, and opening the application of oxazaborine as bright ECL luminophores.

Introduction

Electrogenerated chemiluminescence (ECL) involves the generation of light through an electrochemical stimulus.^[1–4] As analytical technique ECL is far superior to photoluminescence and chemiluminescence in terms of signal to noise ratio and it has been widely used for the ultrasensitive quantification of important biomarkers.^[5–8] The unique propriety of ECL are confirmed by many research applications and by the presence of important companies which developed commercial immuno-assay for clinical analysis worth billions of tests each year.

ECL can be generated by scanning the potential in a range where the luminophore undergoes to heterogeneous electrochemical oxidation and reduction producing radical anion and cation respectively that lead to the formation of the excited states through homogeneous electron transfer. This ECL mechanism is known as annihilation, and is on scheme below: ^[9]



This item was downloaded from IRIS Università di Bologna (<https://cris.unibo.it/>)

When citing, please refer to the published version.

Since the first paper on ECL from Bard and coworkers, Ru(II) polypyridine complexes, in particular the tris(2,2'-bipyridyl) ruthenium (II), [Ru(bpy)₃]²⁺, were the most studied and investigated systems.^{[10][11]} In order to increase sensitivity of ECL assay and tune emission colors significant research efforts have been taken to systematically design and develop functionalized metal based complexes, primarily based on Ru(II) and Ir(III).^[12–19] In fact, common weaknesses for other reported ECL luminophores are often shown in previous researches, thus a limited water solubility,^[20] lack of stability during electrochemical switching,^[13] and the difficulty creating an labelling site without affecting the pristine photophysical/electrochemical properties. On the other hand we recently focused on an insoluble neutral iridium (III) system in aqueous media, which was achieved only with the encapsulation of this compound into silica-polyethylene glycol nanoparticles.^{[21][22]}

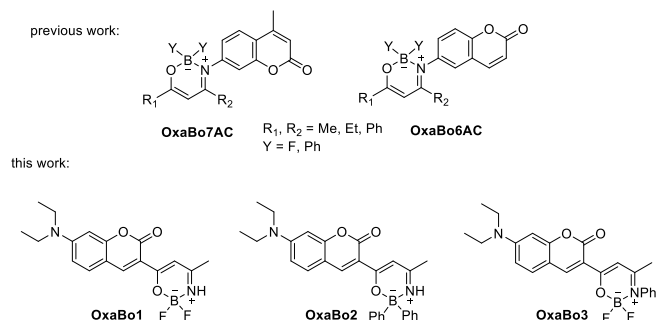
However, the scarcity and high cost of the so-called platinum groups metals requires searching for alternatives. In this context, polycyclic aromatic hydrocarbons are promising options despite their lower intrinsic solubility in water.^[23–26]

Among organic molecules, boron-dipyrromethene (BODIPY) dyes emerged as highly efficient ECL emitters. Bard and co-workers pioneered reported the ECL propriety of various BODIPY derivatives.^[27] BODIPY are a versatile class of luminophores with high fluorescence quantum yields in the visible spectral region and their photophysical properties could be easily modify by tuning the ECL emission wavelength and efficiency.^[28–30] In addition BODIPYs were successfully modified, by Foster and coworker, introducing donor/acceptor groups so as to tune the emission wavelength and increase the Stokes Shift.^[31–33]

Another important class of fluorophores are tetra-coordinated six-membered boron compounds with O–B–N moiety, also called oxazaborines.^[34] These compounds have interesting luminescent properties such as aggregation-induced emission (AIE).^[35] Recently thermally-activated delayed fluorescence (TADF) for a number of these compounds was described.^{[36][37]}

Searching for novel materials having such properties is one of important tasks of modern material chemistry. One approach to the novel materials is a combination of known luminophores.^[38]

Figure 1. Oxazaborines studied previously and in this work.



Recently we have prepared and studied boron ketimines **OxaBo6AC** and **OxaBo7AC** substituted by aminocoumarin fragment on the nitrogen (Figure 1).^[39] Although these compounds possess interesting spectral properties, including relatively long fluorescence lifetimes and AIE, their quantum yield in solution is very poor.

Inspired by the results and for deeper understanding the structure-properties relationships, here, we modified the coumarin-oxazaborine moiety to be directly joined through carbon-carbon bond and form donor–acceptor (D–A) chromophores **OxaBo** with 7-aminocoumarin donor and oxazaborine acceptor. That arrangement can substantially change the electron distribution as well as photophysical, electrochemical and ECL properties with a strong effect on the final quantum yield.

We report the synthesis, electrochemical photophysical and ECL property of this novel class of coumarin-based oxazaborines (compounds **OxaBo1**, **OxaBo2** and **OxaBo3** Figure 1). They were synthesized and characterized in non-aqueous media. All these three novel compounds were analyzed in the same concentration and under the same conditions, according this path, it would be

This item was downloaded from IRIS Università di Bologna (<https://cris.unibo.it/>)

When citing, please refer to the published version.

capable a comparison. Finally, the ECL properties and efficiencies of such compounds have been carried out in aprotic solvent.

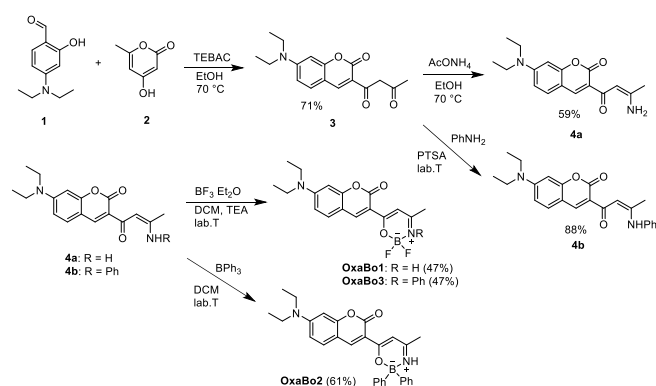
Results and Discussion

Synthesis and NMR Spectroscopy

Oxazaborines studied in this work were prepared via three-stage synthesis shown in Scheme 1. First stage includes condensation between commercially available 4-diethylaminosalicylaldehyde (**1**) and 4-hydroxy-6-methyl-2-pyrone (**2**) giving the starting β -diketone **3** in 71% yield. Diketone **3** has been subjected to the reaction with either ammonium acetate (to give enaminone **4a**) or aniline (to give enaminone **4b**).

Whereas the formation of primary enaminone **4a** proceeded smoothly, the reaction with aniline required long-term heating and azeotropic removal of the reaction water. Regardless of it, the isolated yield of **4b** was very poor (15%). Much better yield (88%) of **4b** was obtained using solvent-free approach. The last step was the chelation of the boron fragment between O, N ligand by means of BF_3 diethyl etherate or triphenylborane. Corresponding oxazaborines **OxaBo** were obtained in moderate yields (40–60%).

The synthesized molecules were fully characterized (see Figs. S1-S10 and experimental section). In addition to that, fluorine-19 NMR spectra of **OxaBo1** and **OxaBo3** (see Figs. S11 and S12) consist of one signal split into 1:1:1:1 quartet via one-bond (^{19}F , ^{11}B) coupling. As was previously observed^[39] this means fast conformational interconversion between the fluorines and the spectra then show their weighted average. Another possibility is planarity or near planarity of the oxazaborine cycle giving the fluorines the symmetric equivalency. The chemical shifts and coupling constants are within the area typical for this kind of compounds.^[39] Boron-11 NMR spectra of **OxaBo1** and **OxaBo3** (Figs. S13, S14) are in accordance with the results obtained by means of ^{19}F NMR. Due to the equivalency of both the fluorines, the boron signals are split into triplets. Their chemical shifts are also typical for those described for tetra-coordinated difluoroboron compounds. On the other hand, the boron signal of **OxaBo2** (Fig. S15), having diphenylboron moiety, is a broad singlet. This was observed also for other similar compounds.^{[40][41][42]} Chemical shift 2.6 ppm lies in the range typical for this kind of compounds and its value also evidences for rather less crowded environment around the boron atom which can be explained by small hydrogen substituent on the nitrogen.^[42]



Scheme 1. Synthesis of **OxaBo**'s.

Electrochemistry

The electrochemical behavior of oxazaborine compounds was studied in acetonitrile containing 0.1M Bu_4NPF_6 as supporting electrolyte. To get consistent information, combination of voltammetric techniques (cyclic voltammetry, rotating disk voltammetry as well as electrode materials: platinum, glassy carbon were employed. The electrochemical data are summarized in table 1.

The first oxidation of all studied compounds proceeds at potentials of +1.01 to +1.07 V (vs SCE) as one-electron reversible process except for compound **OxaBo2**, where the reversibility was observed

This item was downloaded from IRIS Università di Bologna (<https://cris.unibo.it/>)

When citing, please refer to the published version.

at scan rate 8 V s^{-1} and higher. The changes in substitution on oxazaborine core only negligibly influence first oxidation potential, hence when replacing both fluoro substituents by two phenyl groups it causes the shift of first oxidation potential by 60 mV to less positive values.

On the other hand, the first reduction of all three compounds proceeds at potentials of -1.24 to -1.43 V (vs SCE) as irreversible process (see Fig. 2). Nevertheless, at higher scan rates (8 V s^{-1}) the first reduction changes to (quasi)reversible process, this points to the fact that corresponding radical anion has low stability in acetonitrile. When comparing limiting current of the first reduction with limiting current of one-electron oxidation in RDV experiments (see Figs. S16-S18), the ratio 1:1 can be found,

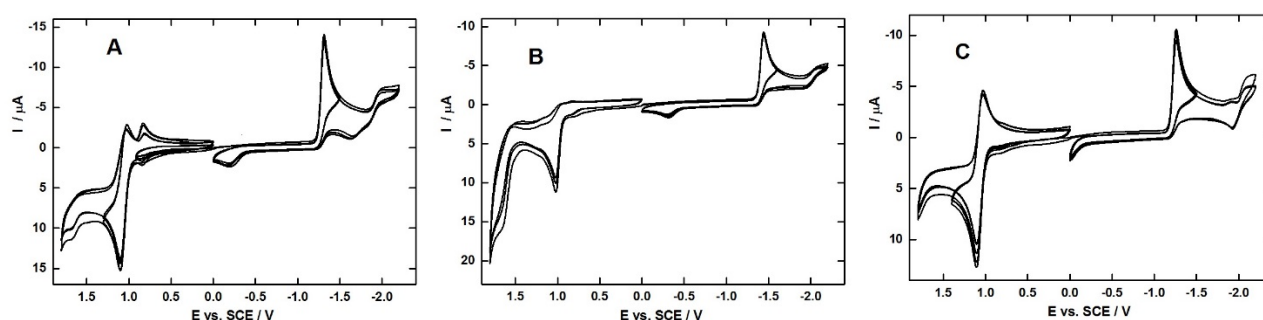


Figure 2. Electrochemical behaviour of **OxaBo 1-3** ($5 \cdot 10^{-4} \text{ M}$) at glassy carbon electrode in CH_3CN ; scan rate $\nu = 100 \text{ mV/s}$.

Table 1. Electrochemical, UV-vis, luminiscence data of studied compounds.

Electrochemistry				Photophysics						ECL	
Compound	$E_{1/2}(\text{ox1})$ [V] vs SCE	$E_{1/2}(\text{red1})$ [V] vs SCE	$E_{\text{ox}} - E_{\text{red}}$ [V]	λ_{max} [nm]	ε [$\text{mol} \cdot \text{dm}^{-3} \cdot \text{cm}^{-1}$]	λ_{exc} [nm]	λ_{em} [nm]	$\Phi_{\text{PL}}[\%]$	τ [ns]	$\lambda_{\text{ECL max}}$ [nm]	Φ_{ECL}
OxaBo 1	1.07	-1.30	2.36	466	70 800	465	518	69 ± 2	1.60	521	0.07
OxaBo 2	1.01	-1.43	2.44	456/471	66 100	463	513	74 ± 1	2.16	-	0.02
OxaBo 3	1.07	-1.24	2.31	478	93 800	478	540	72 ± 3	1.64	553	0.20

which means that the first reduction process consumes one electron. Concerning different substitution on oxazaborine core, when comparing compounds **OxaBo1** and **OxaBo3** with compound **OxaBo2**, the shift of the first reduction potential by about 130-190 mV to less negative values due to presence of electron-withdrawing fluoro substituents can be observed. The easiest reduction process shows compound **OxaBo3**, where the role plays delocalization of electron density as results also from lowest value of first oxidation and reduction potential difference (see tab. 1).

Photophysical properties

UV-vis absorption spectra are in Figure 3 and basic parameters are in Table 1 (see also Fig. S19-21). All the compounds show similar spectra consisting of two main bands 200–203 nm and 456–478 nm. The latter probably attribute to $\pi-\pi^*$ transitions (K-bands, $\log \varepsilon_{\text{max}} = 4.82\text{--}4.97$). The band of **OxaBo2** differ from the others by the shape as it consists of two near bands. It could be due to the presence of another phenyl rings in BPh_2 fragment (another aromatic $\pi-\pi^*$ transition). The bands at ca 200 nm could attribute to ethylenic E-bands due to auxochromic substitution with NEt_2 group.

This item was downloaded from IRIS Università di Bologna (<https://cris.unibo.it/>)

When citing, please refer to the published version.

Compound **OxaBo2** gradually decomposes on standing in diluted solutions (see Fig. S22), hence, the measurements must be done using freshly prepared solutions.

All the studied compounds show strong fluorescence in diluted solutions in acetonitrile with quantum yields around 70% and short fluorescence time constants 1.6–2.16 ns, see the Table 1 and Fig S23. Fluorescence spectra for all compounds in this polar environment shows similar shape without strongly pronounced vibronic progressions suggesting intermolecular charge transfer character of the transitions due to the presence of electron donating dimethylamino group.

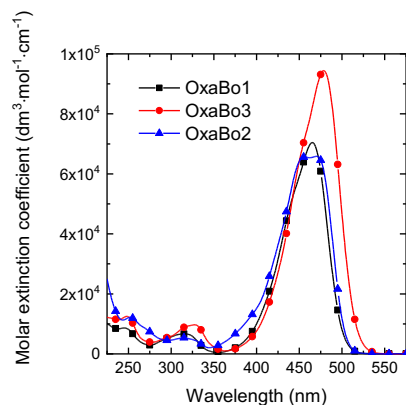


Figure 3 UV-vis spectra of **OxaBo1–3** in CH_3CN (10 μM)

Comparing compounds containing electron withdrawing fluorine atoms (**OxaBo1** and **3**), we can observe clear bathochromic shift in UV-Vis absorption and fluorescence excitation spectra (about 12 nm), and also in fluorescence emission (22 nm) induced by the presence of phenyl on the nitrogen atom. These shifts also translate to increased Stokes shift for **OxaBo3** (62 nm) compared to **OxaBo1** (53 nm). Taking into account the higher molar extinction coefficient of **OxaBo3** than **OxaBo1**, these results seem to indicate that the phenyl causes slightly increased intermolecular charge transfer character.

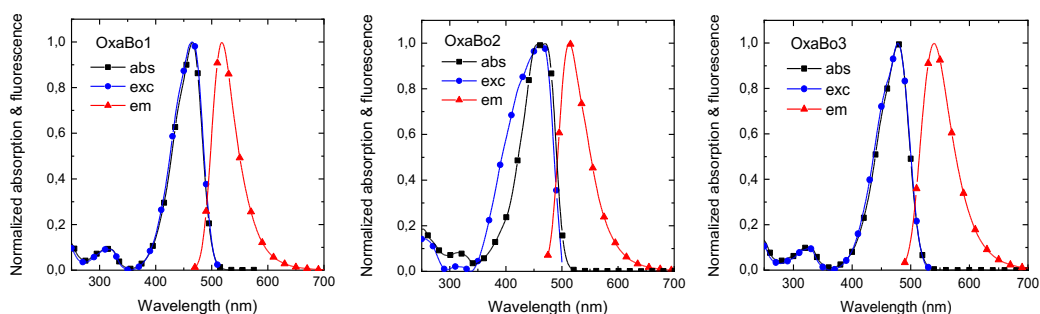


Figure 4 Normalized absorption (squares), fluorescence excitation (circles) and emission (triangles) of the studied coumarin-oxazaborine dyes **OxaBo1**, **OxaBo2**, **OxaBo3**

An opposite behaviour can be observed for compound **OxaBo2** where the fluorine atoms were replaced by phenyls. Comparing **OxaBo2** to the **OxaBo1**, a slight hypsochromic shift was observed for fluorescence excitation and also emission spectra as well as a slightly smaller Stokes shift (50 nm). These observations point to weaker charge transfer character probably due to weaker electron withdrawing moiety.

All these results are summarized in Table 1 and on Figure 4. The optical properties clearly confirm that the directly joined coumarin-oxazaborine moieties allow for efficient intramolecular charge transfer. Further substitutions on these dyes can be used to tune the optical properties such as fluorescence emission wavelength and Stokes shift.

Theoretical study

For deeper insight into UV-Vis absorption properties, the TD-DFT calculations were performed in acetonitrile as a solvent. For the simplification of the calculations the ethyl groups were substituted by methyl groups. The energy levels of HOMO-1, HOMO, LUMO and LUMO+1 together with the orbital locations are depicted in figure 5. Similarly to our previous work^[39] the substitution

This item was downloaded from IRIS Università di Bologna (<https://cris.unibo.it/>)

When citing, please refer to the published version.

of fluorine atoms in **OxaBo1** for phenyl groups in **OxaBo2** causes slight increase of energy of all orbitals and energy gap. Next, introduction of the phenyl substituent on the nitrogen of oxazaborine moiety which is perpendicular to the plane of oxazaborine ring in compound **OxaBo3** has only small effect on orbital distribution. Location of HOMO and LUMO orbitals in different parts of compounds **OxaBo1–3** indicates that an intramolecular charge-transfer (ICT) from dimethylamino group occurs. The results of TD-DFT calculations including oscillator strength values f and the main orbital transitions are summarized in Table 2. The main orbital transitions are attributed to the transitions from the HOMO to LUMO orbitals.

Compound	Transition	Main orbital transition	f
OxaBo1	$S_0 \rightarrow S_1$	HOMO→LUMO	1.17
OxaBo2	$S_0 \rightarrow S_1$	HOMO→LUMO	1.10
OxaBo3	$S_0 \rightarrow S_1$	HOMO→LUMO	1.36

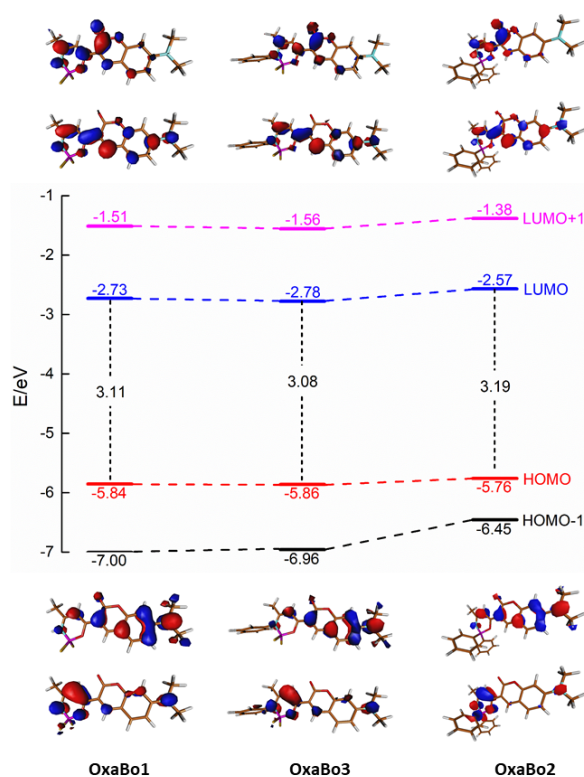


Figure 5. Molecular orbital energy diagram and isodensity surface (contour value 0.04) plots of the HOMO-1, HOMO, LUMO, and LUMO+1 orbitals calculated at the B3LYP/6-311+G** level of theory in CH_3CN .

Electrochemiluminescence

The relatively easy accessibility of the first oxidation and first reduction, and the high photoluminescence efficiency prompted us to study their electrochemiluminescence behavior with the so-called ECL annihilation mechanism. Thus, ECL behavior was tested by chronoamperometry pulse/cyclic voltammetry and the light detection using a photomultiplier tube (PMT), under the same experimental condition previously reported. A platinum side-oriented 2mm diameter disks was used as working electrode, a platinum spiral as counter electrode and as quasi-reference silver wire.

Figure 6 ECL intensity vs potential for 5.10^{-4} M **OxaBo3** (current in black and ECL in red) in $\text{CH}_3\text{CN}/\text{Bu}_4\text{NPF}_6$ (0.1M). Working electrode: Pt disk (2mm diameter) vs SCE electrode with scan rate 1 V s^{-1} . PMT bias of 750V; voltage scan between +1.3 and -1.7

This item was downloaded from IRIS Università di Bologna (<https://cris.unibo.it/>)

When citing, please refer to the published version.

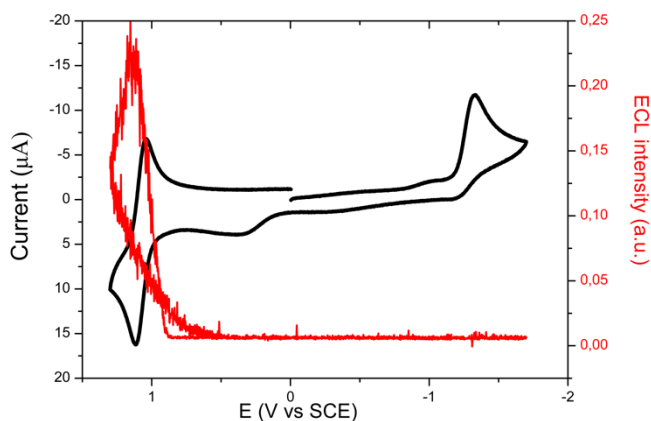
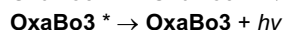
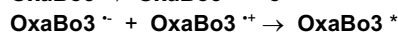
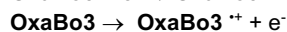
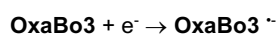


Figure 6 shows the ECL emission that was recorded while cycling the potential between the first reduction and the first oxidation. According to the annihilation mechanism which is shown below, the generation of the excited state is induced by the homogeneous electron transfer between the electrogenerated anion and cation. In fact the emission occurs only when both anion and cation are present with an intensity of 0.22 a.u. with an oxidation current of 17.39 μA (and also Figs. S24 and S25).



The observation of an intense ECL emission, easily visible by the naked eye, confirms the above mechanism. The ECL emission was intense and stable enough to acquire the ECL spectrum reported in figure 7. The spectrum characteristics are similar to PL spectrum with a maximum of emission of 553 nm for **OxaBo3** confirming the generation of the same excited state. ECL spectrum was also recorded for **OxaBo1** while **OxaBo2** ECL emission was not enough intense to acquire reproducible spectrum.

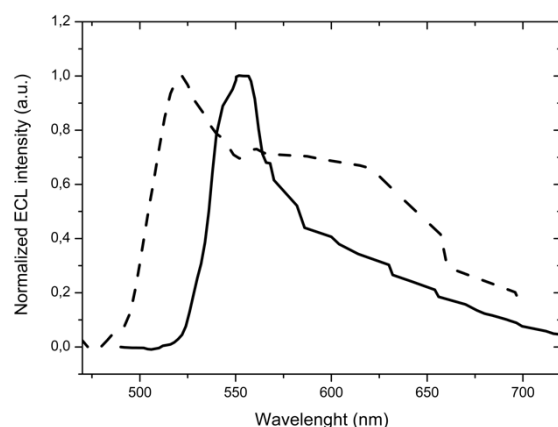


Figure 7 ECL spectra of $5 \cdot 10^{-4}$ M **OxaBo1** (dash line) and **OxaBo3** (solid line) in $\text{CH}_3\text{CN}/\text{Bu}_4\text{NPF}_6$ (0.1M). Working electrode: Pt disk (2mm diameter) vs SCE electrode. PMT bias of 750V; step potential -1.2V; integration time 100s; step 2nm.

Thus, ECL was achieved by the energy-sufficient homogeneous electron transfer occurring between the electrochemically generated molecule radical anion and the radical cation.

Finally, the ECL efficiency can be calculated by the annihilation method and achieved by chronoamperometric techniques under the same experimental conditions, see methods for the detail and Figure S26. [26] The results are reported in Table 1 and show that compound **OxaBo3** yields is ten times higher than the other compounds and almost four times higher than the standard $[\text{Ru}(\text{bpy})_3]^{2+}$.

Conclusion

This item was downloaded from IRIS Università di Bologna (<https://cris.unibo.it/>)

When citing, please refer to the published version.

In summary, we reported the synthesis, electrochemical, photophysical and ECL property of a novel class of coumarin-based oxazaborines. The change in the connection between oxazaborine and coumarin moiety led to a substantially improve in the photophysical properties. Whereas oxazaborines **OxaBo6AC** and **OxaBo7AC** practically do not fluoresce in solution, **OxaBo1–3** show strong fluorescence with $\Phi = 0.69\text{--}0.74$. The change from **OxaBo6AC** and **OxaBo7AC** to **OxaBo1–3** led to a bathochromic shift of the absorption maxima by 100–140 nm and to a smaller HOMO-LUMO gaps (by 0.67–1.35 eV). That can be attributed to higher degree of conjugation in the case of **OxaBo1–3**. These characteristics opened this class of molecules to the application in the field of ECL and result in a very high ECL efficiency, four times higher than the standard dyes. Such oxazaborines could potentially be applied as ECL luminophores in water, and are under investigation in our laboratory, by exploring their aggregation induced properties.

Experimental Section

Electrochemistry. Electrochemical measurements were carried out in acetonitrile containing 0.1M Bu₄NPF₆. Cyclic voltammetry (CV) and rotating disk voltammetry (RDV) were used in a three-electrode arrangement. The working electrode was glassy carbon or platinum disk (2mm in diameter) for CV and RDV experiments. As the reference and auxiliary electrodes were used saturated calomel electrode (SCE) separated by a bridge filled with supporting. All potentials are given vs. SCE. Voltammetric measurements were performed using a potentiostat PGSTAT 128 N (AUTOLAB, Metrohm Autolab B.V., Utrecht, The Netherlands) operated via NOVA 1.11 software.

Electrochemiluminescence. ECL behaviour is controlled by chronoamperometry pulse/cyclic voltammetry and the light detection using a photomultiplier tube (PMT), molecules were carried out with CH₃CN / Bu₄NPF₆ (0.1 M) as supporting electrolyte, under the same aprotic conditions. As working electrode was used a platinum side-oriented 2mm diameter disks sealed in glass while the counter electrode was a platinum spiral and as reference electrode was used a quasi-reference silver wire. These three-electrode system were put in a one-compartment airtight cell, with high-vacuum O-rings and glass stopcocks. The cell was placed a few millimeters from the PMT and in front of the working electrode in the dark-box. The light/current/voltages curves were collected by the PMT output signal (by an ultralow noise Acton research model 181) with the second input channel of the ADC by the AUTOLAB instrument (Ecochemie, Mod. PGSTAT 30).

The ECL efficiency can be meticulously calculated by the annihilation method and achieved by chronoamperometric techniques using the following equation ^[1]

$$\Phi_{\text{ECL}} = \Phi^{\circ}_{\text{ECL}} (I/Q^{\circ}/I^{\circ}Q)$$

Where $\Phi^{\circ}_{\text{ECL}}$ is the ECL efficiency of the standard under the same conditions ($[\text{Ru}(\text{bpy})_3]^{2+}$ $\Phi^{\circ}_{\text{ECL}} = 0.05$), ^[1] I and I° are the integrated ECL intensity of the compounds and the standard system, Q and Q° the faradaic current values passed for the studies compounds and the standard compounds, respectively. In the table1 are presented the ECL efficiencies of each compounds, under the same experimental conditions (Figure S26).

NMR Spectroscopy. NMR Spectra were measured using NMR spectrometers Bruker AVANCE III operating at 400.13 MHz (¹H), 376.50 MHz (¹⁹F), 127.38 MHz (¹B) and 100.12 MHz (¹³C) and Bruker Ascend™ equipped with Cryoprobe™ Prodigy operating at 500.13 MHz (¹H), 470.66 MHz (¹⁹F), 160.48 (¹B) and 125.12 MHz (¹³C). Proton spectra were measured in CDCl₃ and calibrated on an internal TMS ($\delta = 0.00$ ppm). Carbon spectra were measured with broadband proton decoupling. Calibration of the carbon spectra was done on the middle peak of the solvent multiplet ($\delta = 77.23$ ppm). Fluorine-19 NMR spectra were measured without proton decoupling using α,α,α -trifluorotoluene as the secondary external standard^[43] ($\delta = -63.9$ ppm against CFCI₃ as the primary standard). Boron-11 NMR were measured using B(OMe)₃ as an external standard^[44] ($\delta = 18.1$ ppm). All the pulse sequences were taken from the Bruker pulse sequence library. The multiplicity of the signals is expressed as follows: s (singlet), d (doublet), t (triplet), q (quartet), dd (doublet of doublets), m (multiplet), br (broadened signal).

DFT Calculations. The DFT calculations were performed using the density functional method B3LYP^[45]^[46] in conjunction with 6-311+G** basis set as implemented in the Gaussian 09 suite.^[47] The solvent effect was included using CPCM model.^[48] For all optimized structures, frequency analyses at the same level of theory were used to assign them as genuine minima on the potential energy surface. The single point and TD-DFT calculations were performed on the optimized structures on the B3LYP/6-311+G** level of theory.

Optical characterization

UV-vis absorption spectra were measured from freshly prepared solutions ($c = 10^{-5}$ mol·dm⁻³) on a Hewlett-Packard 8453 spectrophotometer and a Varian Cary Probe 50 UV-Vis-NIR spectrometer (Agilent Technologies). The molar extinction coefficients were calculated from the linear part of the concentration dependence of absorption $A=f(c)$, see the Figs S19-21. All optical characteristics were determined in the ambient environment.

The fluorescence spectra and quantum yields were measured using a FS5 Spectrofluorometer (Edinburgh Instruments). The fluorescence quantum yields were determined by means of an absolute method utilizing an integrating sphere. Fluorescence was measured for solutions with absorption below 0.1. Fluorescence lifetimes were measured by means of the TCSPC (Time Correlated Single Photon Counting) method using Horiba JY FluoroCube.

Other characterizations

This item was downloaded from IRIS Università di Bologna (<https://cris.unibo.it/>)

When citing, please refer to the published version.

Elemental analyses were performed on a Flash EA 2000 CHNS automatic analyser (Thermo Fisher Scientific). Their results were found to be in a good agreement ($\pm 0.3\%$) with the calculated values. HRMS were measured on a MALDI LTQ Orbitrap XL (Thermo Fisher Scientific) using 2,5-dihydroxybenzoic acid (DHB) as the matrix. Melting points were measured on a Kofler hot-stage microscope Boetius PHMK 80/2644.

Synthesis

All the solvents and reagents were used commercial without further treatments. Compounds **1** and **2** were commercial (Fluorochem). Triphenylborane was purchased from Strem. Boron trifluoride (ca 48% BF₃) was from Acros. Dry dichloromethane (Acros) was stored under inert using AcroSeal®. Compound **3** was prepared using the procedure published in ref. [49] Yield 71%.

3-(3-Aminobut-2-enoyl)-7-diethylamino-2H-chromen-2-one (4a): A 100 ml round-bottomed flask was charged with compound **3** (3 g, 10 mMol), ammonium acetate (7.7 g, 100 mMol) and ethanol (50 mL). The mixture was refluxed for 1 h. The cooled mixture was then separated between ethyl acetate (130 mL) and water (100 mL) in a separatory funnel. The organic layer was dried over anhydrous sodium sulphate and the volatile components were evaporated in vacuo. The residue was subjected to a column chromatography (silica/DCM-EtOAc 4/1 v/v). Yield 1.77 g (59%) of yellow solid. Rf = 0.18. Mp = 196–197 °C.

¹H NMR (400 MHz, CDCl₃) δ = 10.29 (brs, 1H), 8.49 (s, 1H), 7.38 (d, J = 8.8 Hz, 1H), 6.59 (dd, J = 8.9 Hz; 2.5 Hz, 1H), 6.48 (d, J = 2.3 Hz, 1H), 6.43 (s, 1H), 5.23 (brs, 1H), 3.43 (q, J = 7.1 Hz, 4H), 2.08 (s, 3H), 1.23 (t, J = 7.1 Hz, 6H) ppm.

¹³C NMR (100 MHz, CDCl₃) δ = 184.0; 164.0; 161.0; 157.9; 151.1; 146.3; 131.0; 118.6; 109.5; 108.9; 96.7; 95.6; 45.1; 23.2; 12.6 ppm.

HRMS (MALDI): for C₁₇H₂₀N₂O₃ calcd. [M+H]⁺ 301.15467; [M+Na]⁺ 323.13661; [M+K]⁺ 339.11055; found [M+H]⁺ 301.15441; [M+Na]⁺ 323.13646; [M+K]⁺ 339.11034. Elemental analysis: for C₁₇H₂₀N₂O₃ calcd. C 67.98, H 6.71, N 9.33; found C 68.28, H 6.69, N 9.12.

7-Diethylamino-3-(3-phenylaminobut-2-enoyl)-2H-chromen-2-one (4b): A 25 ml round-bottomed flask was charged with compound **3** (604 mg, 2 mMol), aniline (1.5 mL, 16.5 mMol) and catalytic amount of PTSA (7 mg, 9 mol.%). The mixture was stirred at laboratory temperature for 4 ¼ h. A solid precipitated during this time. The mixture was diluted with EtOH and the precipitate was isolated by suction, washed with ether and dried on air. Yield 663 mg (88%) of orange solid. Mp = 178–180 °C.

¹H NMR (400 MHz, CDCl₃) δ = 13.26 (brs, 1H), 8.53 (s, 1H), 7.41–7.35 (m, 3H), 7.23–7.17 (m, 3H), 6.63 (s, 1H), 6.60 (dd, J = 9.0 Hz, 2.3 Hz, 1H), 6.49 (d, J = 2.0 Hz, 1H), 3.44 (q, J = 7.1 Hz, 4H), 2.17 (s, 3H), 1.23 (t, J = 7.1 Hz, 6H) ppm.

¹³C NMR (100 MHz, CDCl₃) δ = 183.1, 163.1, 160.9, 157.9, 152.2, 146.2, 138.9, 131.0, 129.3, 125.9, 124.9, 118.3, 109.5, 109.0, 97.8, 96.8, 45.2, 20.7, 12.6 ppm.

HRMS (MALDI): for C₂₃H₂₄N₂O₃ calcd. [M+H]⁺ 377.18597; [M+Na]⁺ 399.16791; [M+K]⁺ 415.14185; found [M+H]⁺ 377.18657; [M+Na]⁺ 399.16876; [M+K]⁺ 415.14276. Elemental analysis: for C₁₇H₂₀N₂O₃ calcd. C 73.38, H 6.43, N 7.44; found C 73.18, H 6.40, N 7.36.

General methodology for the synthesis of OxaBo 1 and OxaBo3: A dried flask was charged with enaminone **4** and dry dichloromethane (9mL/mmol). The flask was sealed with a rubber septum, flushed with argon and triethylamine (2 eq.) was added by syringe. Boron trifluoride diethyletherate (3 eq.) was subsequently added dropwise by syringe under stirring at laboratory temperature. The mixture was stirred at laboratory temperature overnight, the volatile components were then evaporated *in vacuo*. The crude residue was dissolved in DCM and washed twice with water. Organic layer was separated, dried over anhydrous sodium sulphate and evaporated to dryness. The residue was separated by column chromatography (see details at individual compounds). The following compounds were prepared:

6-(7-Diethylamino-2-oxo-2H-chromene-3-yl)-2,2-difluoro-4-methyl-1,3,2λ⁴-oxazaborine (OxaBo1): Prepared using the general procedure from 1.49 mmol of **4a**. Chromatography silica DCM:EtOAc 20:1 (v/v), Rf = 0.24 Yield 245 mg (47%) of dark yellow solid, mp = 253–258 °C.

¹H NMR (400 MHz, CDCl₃) δ = 8.69 (s, 1H), 7.42 (d, J = 9.0 Hz, 1H), 7.06 (d, J = 1.8 Hz, 1H), 7.05 (brs, 1H), 6.65 (dd, J = 8.9 Hz, 2.4 Hz, 1H), 6.48 (d, J = 2.2 Hz, 1H), 3.47 (q, J = 7.3 Hz, 4H), 2.33 (s, 3H), 1.25 (t, J = 7.1 Hz, 6H) ppm.

¹³C NMR (125 MHz, CDCl₃) δ = 173.8, 166.8, 159.9, 158.0, 153.2, 147.0, 131.8, 110.7, 110.3, 108.9, 97.1, 96.7, 45.4, 24.6, 12.7 ppm.

¹⁹F NMR (376.5 MHz, CDCl₃) δ = -133.3 (q, ¹J(¹⁹F, ¹B) = 15.1 Hz) ppm.

¹B NMR (128 MHz, CDCl₃) δ = 0.15 (t, ¹J(¹B, ¹⁹F) = 15.1 Hz) ppm.

HRMS (MALDI): for C₁₇H₁₉BF₂N₂O₃ calcd. [M+H]⁺ 349.15296; [M+Na]⁺ 371.13490; [M+K]⁺ 387.10884; found [M+H]⁺ 349.15287; [M+Na]⁺ 371.13484; [M+K]⁺ 387.10878.

Elemental analysis: for C₁₇H₁₉BF₂N₂O₃ calcd. C 58.65, H 5.50, N 8.05; found C 58.80, H 5.52, N 8.07.

6-(7-Diethylamino-2-oxo-2H-chromene-3-yl)-2,2-difluoro-4-methyl-3-phenyl-1,3,2λ⁴-oxazaborine (OxaBo3): Prepared using the general procedure from 1.76 mmol of **4b**. Repeated chromatography on silica, DCM:EtOAc 20:1 v/v Rf = 0.79 and DCM, Rf = 0.59, yield 352 mg (47%) of orange solid, mp = 266–268 °C.

¹H NMR (400 MHz, CDCl₃) δ = 8.71 (s, 1H), 7.47–7.36 (m, 4H), 7.26–7.25 (m, 2H), 7.17 (s, 1H), 6.65 (dd, J = 8.7 Hz, 2.3 Hz, 1H), 6.49 (d, J = 2.3 Hz, 1H), 3.47 (q, J = 7.3 Hz, 4H), 2.08 (s, 3H), 1.25 (t, J = 7.1 Hz, 6H) ppm.

¹³C NMR (125 MHz, CDCl₃) δ = 172.3, 165.0, 159.9, 158.0, 153.2, 146.7, 140.3, 131.7, 129.5, 128.3, 126.4, 110.9, 110.2, 108.9, 99.1, 96.7, 45.4, 22.3, 12.7 ppm.

¹⁹F NMR (376.5 MHz, CDCl₃) δ = -136.6 (q, ¹J(¹⁹F, ¹B) = 15.2 Hz) ppm.

¹B NMR (128 MHz, CDCl₃) δ = 0.56 (t, ¹J(¹B, ¹⁹F) = 15.6 Hz) ppm.

HRMS (MALDI): for C₂₃H₂₃BF₂N₂O₃ calcd. [M+H]⁺ 425.18426; [M+Na]⁺ 447.16620; [M+K]⁺ 463.14014; found [M+H]⁺ 425.18477; [M+Na]⁺ 447.16684; [M+K]⁺ 463.14085.

Elemental analysis: for C₂₃H₂₃BF₂N₂O₃ calcd. C 65.11, H 5.46, N 6.60; found C 64.83, H 5.57, N 6.69.

This item was downloaded from IRIS Università di Bologna (<https://cris.unibo.it/>)

When citing, please refer to the published version.

6-(7-Diethylamino-2-oxo-2H-chromene-3-yl)-4-methyl-2,2-diphenyl-1,3,2λ⁴-oxazaborine (OxaBo2): A dried flask was charged with enaminone **4a** (428 mg g, 1.42 mMol) and triphenylborane (518 mg, 2.14 mMol). The flask was sealed with septum, flushed with argon and dichloromethane (10 mL) was added through syringe. The mixture was stirred at laboratory temperature for 24 h. The mixture was then filtered through filter glass and the filtrate was evaporated to dryness *in vacuo*. The residue was subjected to column chromatography (silica, DCM). R_f = 0.28 Yield 407 mg (61%) of orange solid, mp = 251–256 °C.

¹H NMR (400 MHz, CDCl₃): δ = 8.67 (s, 1H), 7.45–7.43 (m, 4H), 7.38 (d, J = 8.9 Hz, 1H), 7.29–7.25 (m, 4H), 7.23–7.18 (m, 2H), 7.00 (brs, 1H), 6.80 (s, 1H), 6.58 (dd, J = 9.0 Hz, 2.2 Hz, 1H), 6.44 (d, J = 1.9 Hz, 1H), 3.42 (q, J = 7.5 Hz, 4H), 2.21 (s, 3H), 1.21 (t, J = 7.1 Hz, 6H) ppm.

¹³C NMR (125 MHz, CDCl₃): δ = 170.5, 167.0, 160.1, 157.8, 152.6, 150.7 (br), 146.0, 132.1, 131.4, 127.4, 126.4, 112.7, 109.9, 109.0, 97.4, 96.7, 45.3, 24.8, 12.7 ppm.

¹¹B NMR (128 MHz, CDCl₃): δ = 2.60 ppm (br).

HRMS (MALDI): for C₂₉H₂₉BN₂O₃ calcd. [M+H]⁺ 465.23340; [M+Na]⁺ 487.21634; found [M+H]⁺ 465.23486; [M+Na]⁺ 487.21703.

Acknowledgements

This work is supported by the Italian Ministero dell'Istruzione, Università e Ricerca (FIRB RBAP11C58Y, PRIN-2010N3T9M4, PRIN-2017FJCPEX, 2017PBXPN4, FIRB RBAP11-ETKA_006), University of Bologna, INSTM and by Czech Science Agency via project No GA17-21105S.

Keywords: Electrochemiluminescence • Molecular electrochemistry • oxazaborines • donor–acceptor chromophores

- [1] W. Miao, *Chem. Rev.* **2008**, 2506–2553.
- [2] J. A. Bard, Ed. , *Electrogenerated Chemiluminescence*, Marcel Dekker, New York, **2004**.
- [3] M. Hesari, Z. Ding, *J. Electrochem. Soc.* **2016**, 163, H3116–H3131.
- [4] Q. Zhai, J. Li, E. Wang, *ChemElectroChem* **2017**, 4, 1639–1650.
- [5] A. L. Jones, L. Dhanapala, R. Kankanamage, C. V. Kumar, J. F. Rusling, *Anal Chem* **2019**, DOI: 10.10, DOI 10.1021/acs.analchem.9b05080.
- [6] Z. Liu, W. Qi, G. Xu, *Chem. Soc. Rev.* **2015**, 44, 3117–3142.
- [7] A. Juzgado, A. Soldà, A. Ostric, A. Criado, G. Valenti, S. Rapino, G. Conti, G. Fracasso, F. Paolucci, M. Prato, *J. Mater. Chem. B* **2017**, 5, 6681–6687.
- [8] G. Valenti, E. Rampazzo, S. Kesarkar, D. Genovese, A. Fiorani, A. Zanut, F. Palomba, M. Marcaccio, F. Paolucci, L. Prodi, *Coord. Chem. Rev.* **2018**, 367, 65–81.
- [9] A. Kapturkiewicz, *ChemElectroChem* **2017**, 4, 1604–1638.
- [10] Y. Yuan, S. Han, L. Hu, S. Parveen, G. Xu, *Electrochim. Acta* **2012**, 82, 484–492.
- [11] W. Miao, J. P. Choi, A. J. Bard, *J. Am. Chem. Soc.* **2002**, 124, 14478–14485.
- [12] A. Fiorani, G. Valenti, M. Iurlo, M. Marcaccio, F. Paolucci, *Curr. Opin. Electrochem.* **2018**, 8, 31–38.
- [13] B. D. Muegge, M. M. Richter, *Anal. Chem.* **2004**, 76, 73–77.
- [14] A. Kapturkiewicz, *Anal. Bioanal. Chem.* **2016**, 7013–7033.
- [15] E. Kerr, E. H. Doeven, G. J. Barbante, T. U. Connell, P. S. Donnelly, D. J. D. Wilson, T. D. Ashton, F. M. Pfeffer, P. S. Francis, *Chem. Eur. J.* **2015**, 21, 14987–14995.
- [16] L. C. Soulsby, D. J. Hayne, E. H. Doeven, D. J. D. Wilson, J. Agugiaro, T. U. Connell, L. Chen, C. F. Hogan, E. Kerr, J. L. Adcock, et al., *Phys. Chem. Chem. Phys.* **2018**, 20, 18995–19006.
- [17] L. Chen, D. J. Hayne, E. H. Doeven, J. Agugiaro, D. J. D. Wilson, L. C. Henderson, T. U. Connell, Y. H. Nai, R. Alexander, S. Carrara, et al., *Chem. Sci.* **2019**, 10, 8654–8667.

This item was downloaded from IRIS Università di Bologna (<https://cris.unibo.it/>)

When citing, please refer to the published version.

- [18] E. Kerr, E. H. Doeven, G. J. Barbante, C. F. Hogan, D. J. Bower, P. S. Donnelly, U. Connell, P. S. Francis, *Chem. Sci.* **2014**, 6, 472–479.
- [19] K. N. Swanick, M. Sandroni, Z. Ding, E. Zysman-colman, *Chem. Eur. J.* **2015**, 7435–7440.
- [20] S. Zanarini, M. Felici, G. Valenti, M. Marcaccio, L. Prodi, S. Bonacchi, P. Contreras-Carballada, R. M. Williams, M. C. Feiters, R. J. M. Nolte, et al., *Chem. Eur. J.* **2011**, 17, 4640–4647.
- [21] S. Kesarkar, E. Rampazzo, G. Valenti, M. Marcaccio, A. Bossi, L. Prodi, F. Paolucci, *ChemElectroChem* **2017**, 4, 1690–1696.
- [22] S. Kesarkar, S. Valente, A. Zanut, F. Palomba, A. Fiorani, M. Marcaccio, E. Rampazzo, G. Valenti, F. Paolucci, L. Prodi, *J. Phys. Chem. C* **2019**, 123, 5686–5691.
- [23] H. Li, J. Daniel, J. B. Verlhac, M. Blanchard-Desce, N. Sojic, *Chem. Eur. J.* **2016**, 22, 12702–12714.
- [24] F. Rizzo, F. Polo, G. Bottaro, S. Fantacci, S. Antonello, L. Armelao, S. Quici, F. Maran, *J. Am. Chem. Soc.* **2017**, 139, 2060–2069.
- [25] H. Li, S. Voci, A. Wallabregue, C. Adam, G. M. Labrador, R. Duwald, I. Hernández Delgado, S. Pascal, J. Bosson, J. Lacour, et al., *ChemElectroChem* **2017**, 4, 1750–1756.
- [26] G. Valenti, A. Fiorani, S. Di Motta, G. Bergamini, M. Gingras, P. Ceroni, F. Negri, F. Paolucci, M. Marcaccio, *Chem. Eur. J.* **2015**, 21, 2936–2947.
- [27] A. B. Nepomnyashchii, A. J. Bard, *Acc. Chem. Res* **2012**, 45, 1844–1853.
- [28] A. B. Nepomnyashchii, M. Bröring, J. Ahrens, A. J. Bard, *J. Am. Chem. Soc.* **2011**, 133, 8633–8645.
- [29] H. Qi, J. J. Teesdale, R. C. Pupillo, J. Rosenthal, A. J. Bard, *J. Am. Chem. Soc.* **2013**, 135, 13558–13566.
- [30] M. Hesari, J.-S. Lu, S. Wang, Z. Ding, *Chem. Commun.* **2015**, 51, 1081–4.
- [31] A. Venkatanarayanan, A. Martin, T. E. Keyes, R. J. Forster, *Electrochem. Commun.* **2012**, 21, 46–49.
- [32] A. Martin, C. Long, R. J. Forster, T. E. Keyes, *Chem. Commun.* **2012**, 48, 5617–5619.
- [33] A. Venkatanarayanan, A. Martin, K. M. Molapo, E. I. Iwuoha, T. E. Keyes, R. J. Forster, *Electrochem. Commun.* **2013**, 31, 116–119.
- [34] D. Frath, J. Massue, G. Ulrich, R. Ziessel, *Angew. Chem. Int. Ed.* **2014**, 53, 2290–2310.
- [35] J. Mei, N. L. C. Leung, R. T. K. Kwok, J. W. Y. Lam, B. Z. Tang, *Chem. Rev.* **2015**, 115, 11718–11940.
- [36] D. Zhou, D. Liu, X. Gong, H. Ma, G. Qian, S. Gong, G. Xie, W. Zhu, Y. Wang, *ACS Appl. Mater. Interfaces* **2019**, 11, 24339–24348.
- [37] G. Li, W. Lou, D. Wang, C. Deng, Q. Zhang, *ACS Appl. Mater. Interfaces* **2019**, 11, 32209–32217.
- [38] X. Liu, Z. Xu, J. M. Cole, *J. Phys. Chem. C* **2013**, 117, 16584–16595.
- [39] H. Doušová, N. Almonasy, T. Mikysek, J. Váňa, M. Nepraš, B. Frumarová, M. Dvořák, Z. Růžicková, P. Šimůnek, *Monatsh. Chem.* **2018**, 149, 1795–1811.
- [40] M. Pešková, P. Šimůnek, V. Bertolasi, V. Macháček, A. Lyčka, *Organometallics* **2006**, 25, 2025–2030.
- [41] M. Svobodová, J. Bárta, P. Šimůnek, V. Bertolasi, V. Macháček, *J. Organomet. Chem.* **2009**, 694, 63–71.
- [42] H. Doušová, P. Šimůnek, N. Almonasy, Z. Růžicková, *J. Organomet. Chem.* **2016**, 802, 60–71.
- [43] K. H.-O. Berger S, Braun S, *NMR Spectroscopy of the Non-Metallic Elements*, Wiley, Chichester, **1997**.
- [44] K. JD, *Boron in Multinuclear NMR*, New York, **1987**.
- [45] S. H. Vosko, L. Wilk, M. Nusair, *J Phys* **1980**, 58, 1200–1211.
- [46] A. D. Becke, *J Chem Phys* **1993**, 98, 5648–5652.
- [47] D. J. Frisch, M. J.; Trucks, G. W.; Schlegel, H. B.; Scuseria, G. E.; Robb, M. A.; Cheeseman, J. R.; Scalmani, G.; Barone, V.; Mennucci, B.;

This item was downloaded from IRIS Università di Bologna (<https://cris.unibo.it/>)

When citing, please refer to the published version.

Petersson, G. A.; Nakatsuji, H.; Caricato, M.; Li, X.; Hratchian, H. P.; Izmaylov, A. F.; Bloino, J.; Zheng, G.; Sonnenb, **2009**.

[48] M. Cossi, N. Rega, G. Scalmani, V. Barone, *J Comput Chem* **2003**, *24*, 669–681.

[49] W. J. Xu, D. Q. Qi, J. Z. You, F. F. Hu, J. Y. Bian, C. X. Yang, J. Huang, *J. Mol. Struct.* **2015**, *1091*, 133–137.

This item was downloaded from IRIS Università di Bologna (<https://cris.unibo.it/>)

When citing, please refer to the published version.